SBA-15-supported poly(4-styrenesulfonyl(perfluorobutylsulfonyl)imide) as heterogeneous Brønsted acid catalyst for synthesis of diindolylmethane derivatives

Zhong-Hua Ma [a,b], Hong-Bo Han [a], Zhi-Bin Zhou [a], Jin Nie [a,*]

[a] *School of Chemistry and Chemical Engineering, Huazhong University of Science and Technology, Wuhan 430074, PR China*
[b] *Department of Chemistry, College of Basic Sciences, Huazhong Agricultural University, Wuhan 430070, PR China*

ARTICLE INFO

ABSTRACT

By means of immobilizing the acidic homopolymer, poly(4-styrenesulfonyl(perfluorobutylsulfonyl)imide) (PSFSI), onto SBA-15 silica, a new type of strongly acidic composite catalyst was developed. The properties of the catalyst were characterized by NMR, FT-IR, XRD, SEM, TEM, XPS, TG, and GPC. The solid acid catalyst was highly effective and could be recycled at least five times without obvious loss of activity for the condensation of indole with structurally diverse aldehydes, which yielded diindolylmethane derivatives (DIMs).

1. Introduction

Among various indole analogs, diindolylmethane derivatives (DIMs) display versatile biological and pharmacological activities [1,2]. They are useful in the treatment of fibromyalgia, chronic fatigue and irritable bowel syndrome [3,4], and as dietary supplements for promoting healthy estrogen metabolism in humans [5], and also effective in the prevention of cancer [6,7].

Despite the fact that various derivatives have been isolated from natural sources [8], the experimental studies on manual synthesis of the DIMs remain important. Both Lewis acids and Brønsted acids can catalyze the electrophilic substitution reaction of indole with aldehydes/ketones to afford DIMs. Over a past few years, several catalyst systems have been reported, such as lanthanide triflates [9], InCl$_3$ [10], LiClO$_4$ [11], Zn^{2+} ion-exchanged Y zeolite [6], montmorillonite K10 clay [12], ionic liquids with FeCl$_3$ [13], NaHSO$_4$·SiO$_2$/Amberlyst 15 [14], Zeokarb-225 [15], HClO$_4$–SiO$_2$ [3] and macroreticular FPS resins [16]. Although some of these catalysts are promising, there is still a need to develop a new type of effective catalyst for the synthesis of DIMs.

Recently, the supported solid Brønsted acid catalysts containing perfluoroalkylsulfonyl groups have received considerable attention in the development of new solid Brønsted acid catalysts [17–21] because of the high acid strength [22,23]. In the present work, we immobilized an acidic homopolymer, poly(4-styrenesulfonyl(perfluorobutylsulfonyl)imide) (PSFSI), onto the popular silica sieve SBA-15 [24,25] to develop a new type of strongly acidic composite catalyst and its catalytic activity was investigated for the synthesis of DIMs under mild reaction conditions.

2. Experimental

2.1. Materials

All solvents (A.R.) for synthesis were commercially available in China and pretreated before used. Sodium 4-styrenesulfonate (industrial grade) was obtained from XZL Chemicals Co., Ltd. (China) and dried beforehand. NKC-9 resin, purchased from Nankai Chemical Plant, was soaked in ethanol, which was renewed every 5 h until it looked colorless. The resin was acidified with 5–10% of HCl and then water scrubbed until no Cl$^-$ ion could be detected (acid loading = 4.74 mmol/g).

2.2. Characterization of catalyst

XRD patterns were recorded on a Bruker D8 X-ray powder diffractometer with Cu Kα (1.54 Å) radiation at 0.5–5° (2θ)
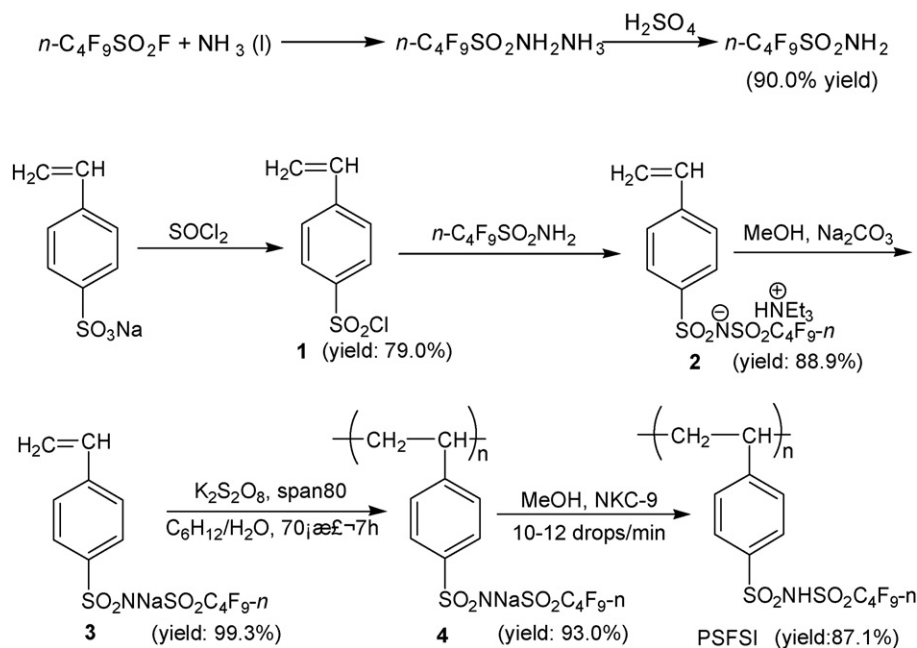
Scheme 1. Synthesis route of linear PSFSI.

angles. The molecular weights of homopolymers were readily determined by GPC on a PL aquagel-OH MIXED column (8 μm, 300 mm × 7.5 mm) equipped with a refractive index signal detector. The GPC system was calibrated with polyethylene oxide, and ran with water as eluent at a flow rate of 1.0 mL/min. FT-IR spectra were conducted by using an Avatar 330 Fourier Spectrometer with the KBr pellet technique. NMR was recorded in DMSO-d_6 solution on a Bruker AV400 spectrometer using TMS and Cl_3CF as the internal standard, respectively. Transmission electron microscopy (TEM) was performed with a HITACHI H-7000FA EM at an acceleration voltage of 75 kV. SEM pictures of the sample surface were obtained by using a Srion 200 (FEI Company) field-transmitting scanning electron microscope equipment and the sample surface was decorated by a thin gold layer with a 682 device (Gatan Inc.) before imaging. Thermogravimetric analysis (TGA) was carried out on a TG209 (Netzsch.) instrument at a heating rate of 20 °C/min under air atmosphere. X-ray photoelectron spectra (XPS) were measured on a VG Multilab2000 X-ray spectrometer equipped with a hemispherical electron analyzer and an Al anode X-ray exciting source (Al Kα energy = 1486.6 eV).

2.3. Synthesis of poly(4-styrenesulfonyl(perfluorobutylsulfonyl)imide) (PSFSI)

The synthesis route of the linear homopolymer is shown in Scheme 1. $C_4F_9SO_2NH_2$ and 4-styrenesulfonyl chloride (**1**) were prepared according to the literature [20,21] and [26,27], respectively. Compound **1** was purified by column chromatography with petroleum ether as eluent, and stabilized by addition of a trace of t-butylcatechol [28].

2.3.1. Synthesis of sodium 4-styrenesulfonyl(perfluorobutylsulfonyl)imide (**3**)

Compound **2** was synthesized according to the modified protocol reported by Hofmann et al. [29]. 1,2-Dichloroethane (DCE) was used as reaction solvent and the reaction was carried out at 70 °C. The crude product was purified by flash chromatography on a silica column. Elution with ether was used to selectively

remove impurities, sequentially with methanol to give product **2**. The partly concentrated methanol solution of **2** was treated with excess Na_2CO_3 powder to yield sodium salt **3**. Agitation lasted for 8 h at room temperature and **3** (buff, yield: 99%) could be readily obtained after centrifugation and evaporation. No inhibitor was necessary. The ^1H NMR spectrum of **3** is shown in Fig. 1(a). IR (KBr, υ, cm^{-1}): 3096, 3070 (–CH_2=CH<), 1400 (–SO_2NHSO_2–), 1330–1145 (–$CF_2CF_2CF_3$); ^{19}F NMR (ppm): −80.82 (3F, CF_3), −112.57 (2F, CF_2SO_2), −121.19 (2F, CF_2), −125.98 (2F, CF_2).

Compound **2** (yellow liquid, yield: 89%) could be obtained by evaporating the solvent with an addition of a trace of t-butylcatechol as the inhibitor and no polymerization happened meanwhile. IR (KBr, υ, cm^{-1}): 3093, 1631 (–CH_2=CH<), 1398 (–SO_2NHSO_2–), 1327–1142 (–$CF_2CF_2CF_3$); ^1H NMR ($CDCl_3$): 7.457–7.901 (m, 4H, –C_6H_4–), 6.695–6.766 (m, 1H, CH), 5.359–5.859 (m, 2H, CH_2), 3.195–3.249 (m, 6H, NCH_2), 1.132–1.523 (t, 9H, CH_2CH_3).
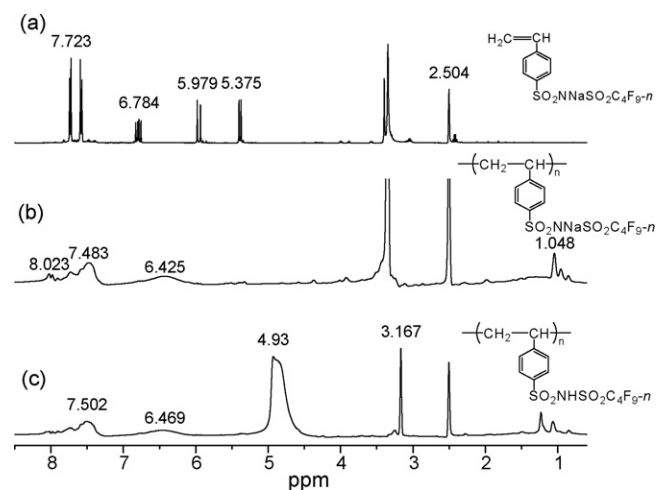

Fig. 1. ^1H NMR spectra of: (a) p-CH_2=$CHC_6H_4SO_2NNaSO_2C_4F_9$ (**3**); (b) Polymer of sodium salt (**4**); (c) PSFSI.
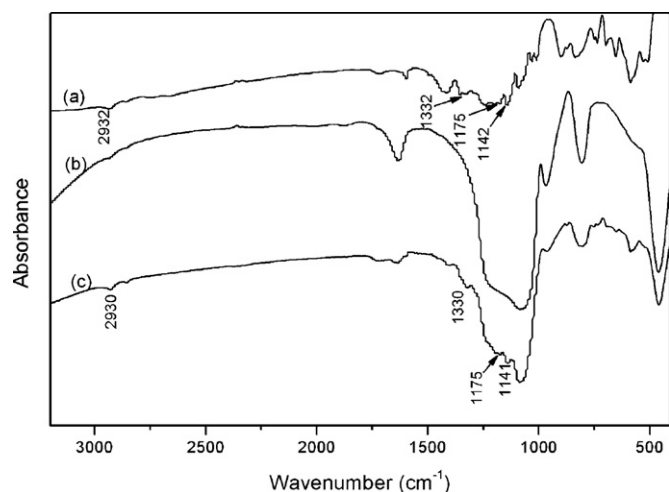
Fig. 2. FT-IR spectra of: (a) PSFSI; (b) SBA-15; (c) PSFSI/SBA-15.

2.3.2. Synthesis of poly(4-styrenesulfonyl(perfluorobutylsulfonyl)imide) (PSFSI)

Aforesaid monomer **3** (10 g, 20.53 mmol) dissolved in 8 mL of distilled water was added into 50 mL of clear cyclohexane containing Span-80 (1.218 g) at 40 °C with stirring, and the mixture was sequently heated to 70–75 °C. Another 2 mL of distilled water containing 0.164 g $K_2S_2O_8$ was carefully added dropwise under nitrogen atmosphere. The homopolymerization was performed for 6 h. After cooled, filtered off, washed with DCE and dried under vacuum, the buff solid **4** (yield: 93%) was obtained. The ^1H NMR spectrum of **4** is shown in Fig. 1(b). IR (KBr, υ, cm^{-1}): 2932, 2857 (polymer main chain), 1417, 1354 (–SO$_2$NHSO$_2$–), 1329–1143 (–CF$_2$CF$_2$CF$_2$CF$_3$).

5.2 g of **4** was dissolved in 20 mL methanol and stirred at 40 °C for at least 8 h for entire solvation. Then, ionic exchange was carried out with approximately 20 g of NKC-9 resin at the flow rate of 12 drops/min until the eluent showed no acidity when detected by pH paper. The concentrated solution of PSFSI could be directly used in the next step, or evaporated to yield a yellow residue. The ^1H NMR spectrum of PSFSI is shown in Fig. 1(c) and the IR spectrum in Fig. 2(a).

2.4. Synthesis of SBA-15 silica

The pure SBA-15 support was synthesized by adopting a method suggested by Choi et al. [24,25]. A stoichiometric amount of white powder was obtained.

2.5. Immobilization of PSFSI onto SBA-15

A wet impregnation technique was used for the immobilization of PSFSI [30]. SBA-15 support was introduced into a three-neck flask containing anhydrous methanol. Methanol solution of PSFSI was then added. The slurry was continuously stirred at room temperature for 6 h, and then solvent was removed by rotary evaporation

under reduced pressure. In the end, the resultant solid was dried at 135 °C overnight. The mass ratio of the initial mixture was 1:1.15 and 1:1 (PSFSI: SBA-15, wt/wt), and the corresponding catalysts were designated as PSFSI$_1$/SBA-15 and PSFSI$_2$/SBA-15, respectively.

2.6. Measurement of acid strength and contents for PSFSI/SBA-15

The acid-exchange capacity was determined by titration with NaOH [31,32]. Typically, 0.3 g of solid was added to 50 mL of 1 mol/L aqueous NaCl solution. The suspension was stirred at room temperature for 24 h until equilibrium was reached, and subsequently titrated by dropwise addition of 0.020 mol/L NaOH solution with phenolphthalein as indicator. The conclusive loading of the PSFSI/SBA-15 was determined by several parallel experiments.

The acid strength of PSFSI$_1$/SBA-15 was characterized by the Hammett indicator method [20,21]. The PSFSI$_1$/SBA-15 was pretreated in vacuum at 130 °C for 5 h, and then allowed to be in contact with the vapor of the Hammett indicator. The acid strength was determined by observing the color change of indicator adsorbed on the surface of the PSFSI$_1$/SBA-15. The anthraquinone ($H_0 = -8.2$), *p*-nitrotoluene ($H_0 = -11.35$) and 4-chloronitrobenzene ($H_0 = -12.70$) were used as indicators and refined benzene was used as the solvent.

2.7. Catalytic reactions

The reactions of indole (4 mmol) and aromatic aldehyde (2 mmol) or aliphatic aldehyde (3 mmol) were carried out for an appropriate period (monitored by TLC) at room temperature in the presence of 0.1149 g (5 mol%) of PSFSI$_1$/SBA-15 with 8 mL of dichloromethane (DCM) as a solvent. After completion of the reaction, filtration was performed and the catalyst was washed thoroughly with DCM. The combined washings and the filtrate were evaporated in vacuum. The obtained residue was purified by column chromatography and eluted with ethyl acetate and petroleum ether mixture. The products (**5a–q**) were identified with FT-IR, ^1H NMR, and LC–MS. The recovered catalyst was dried at 100 °C under vacuum and reused for the next run. The general reaction is given in Scheme 2.

The NMR and IR spectral data of the products (**5a–q**):

3,3′-*Bis*(indolyl)phenylmethane (**5a**) IR (KBr, υ, cm^{-1}): 3410 (NH), 3054, 2956 (CH, υ_{as}), 2854 (CH, υ_s), 1454 (C=N), 743 (NH, γ); ^1H NMR (400 Mz, CDCl$_3$) δ: ~7.93(s, 2H, NH), 7.394–7.367 (m, 6H), 7.320–7.303 (m, 2H), 7.249–7.209 (m, 3H, ^3J = 8 Hz), 7.191–7.171 (m, 2H, ^3J = 8 Hz), 7.044–7.006 (t, 2H), 6.694–6.691 (d, 2H), 5.914 (s, 1H, Ar-CH).

3,3′-*Bis*(indolyl)-4-nitrophenylmethane (**5b**) (KBr, υ, cm^{-1}): 3456, 3423 (NH), 3386, 3052, 1507 (NO$_2$, υ_{as}), 1456 (C=N), 1339 (NO$_2$, υ_s), 746 (NH, γ); ^1H NMR (400 Mz, DMSO-d_6) δ: 10.938–10.934(d, 2H, NH), 8.164–8.142 (d, 2H, ^3J = 8.8 Hz), 7.622–7.601 (d, 2H, ^3J = 8.8 Hz), 7.374–7.354 (d, 2H, ^3J = 8 Hz), 7.297–7.277 (d, 2H, ^3J = 8 Hz), 7.071–7.035 (m, 2H, ^3J = 7.2 Hz), 6.901–6.865 (m, 4H, ^3J = 7.2 Hz), 6.029 (s, 1H, Ar-CH).

3,3′-*Bis*(indolyl)-3-nitrophenylmethane (**5c**) (KBr, υ, cm^{-1}): 3410 (NH), 3055, 1525 (NO$_2$, υ_{as}), 1456 (C=N), 1348 (NO$_2$, υ_s), 743
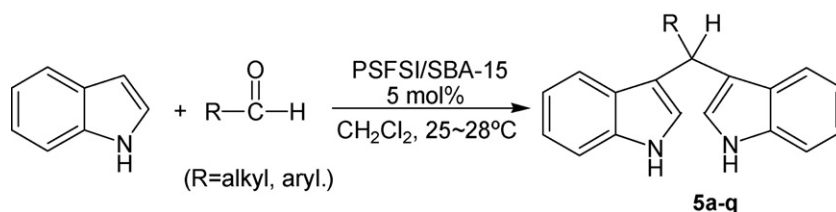
Scheme 2. Condensation of indole with aldehydes.

(NH, γ); ^{1}H NMR (400 Mz, DMSO-d_6) δ: 10.915 (s, 2H, NH), 8.077–8.057 (d, 1H, [3]J = 8.0 Hz), 7.848–7.829 (d, 1H, [3]J = 7.6 Hz), 7.605–7.566 (t, 1H, [3]J = 8.0 Hz, [3]J = 7.6 Hz), 7.397–7.359 (d, 2H [3]J = 8.0 Hz), 7.312–7.292 (d, 2H, [3]J = 8.0 Hz), 7.076–7.039 (t, 2H, [3]J = 7.2 Hz, [3]J = 7.6 Hz), 6.903–6.867 (t, 4H, [3]J = 7.2 Hz, [3]J = 7.6 Hz), 6.065 (s, 1H, Ar-CH).

2,4-*Dichlorophenyl*-3,3′-*bis*(*indolyl*)*methane* (**5d**) (*KBr, ν, cm*$^{-1}$): 3412 (NH), 3050, 2950, 2914, 2849, 1456, 1418, 1383, 1337, 1095, 741; ^{1}H NMR (400 Mz, CDCl$_3$) δ: 7.959 (s, 2H, NH), 7.446–7.440 (d, 1H), 7.384–7.362 (m, 4H), 7.209–7.160 (m, 3H), 7.139 (s, 1H), 7.098–7.009 (m, 2H), 6.652–6.644 (m, 2H), 6.276 (s, 1H).

2-*Chlorophenyl*-3,3′-*bis*(*indolyl*)*methane* (**5e**) (*KBr, ν, cm*$^{-1}$): 3411 (NH), 3055 (C–H, υ), 2957, 2921, 1456 (C=N), 1417, 1337, 742 (NH, γ); ^{1}H NMR (400 Mz, DMSO-d_6) δ: 10.865 (s, 2H, NH), 7.478–7.458 (m, 1H), 7.375–7.354 (d, 2H), 7.285–7.194 (m, **5H**), 7.072–7.034 (t, 2H, [3]J = 7.6 Hz), 6.902–6.864 (t, 2H, [3]J = 7.6 Hz), 6.759 (s, 2H), 6.215 (s, 2H).

3,3′-*Bis*(*indolyl*)-3-*methylphenylmethane* (**5f**) (*KBr, ν, cm*$^{-1}$): 3409 (NH), 3052 (C–H, υ), 2950, 2920, 2856, 1455 (C=N), 1416, 1337, 1092, 771, 742 (NH, γ); ^{1}H NMR (400 Mz, DMSO-d_6) δ: 10.798 (s, 2H, NH), 7.348–7.327 (d, 2H, [3]J = 8.4 Hz), 7.288–7.268 (d, 2H, [3]J = 8.4 Hz), 7.188 (s, 1H), 7.147–7.135 (m, 2H), 7.044–7.007 (m, 2H, J = 7.6 Hz), 6.985–6.976 (t, 1H), 6.874–6.837 (m, 2H, J = 7.6 Hz), 6.816–6.811 (m, 2H), 5.774 (s, 1H, Ar-CH), 2.234 (s, 3H, Ar-CH$_3$).

3,3′-*Bis*(*indolyl*)-4-*methoxyphenylmethane* (**5g**) (*KBr, ν, cm*$^{-1}$): 3395 (NH), 3054 (C–H, υ), 2947, 2921, 2831, 1509, 1455 (C=N), 1023 (ArOC, υ), 784, 741 (NH, γ); ^{1}H NMR (400 Mz, DMSO-d_6) δ: 10.784 (s, 2H, NH), 7.345–7.324 (d, 2H, [3]J = 8.4 Hz), 7.271–7.237 (d, 4H, [3]J = 8.4 Hz, [3]J = 7.6 Hz), 7.040–7.004 (m, 2H, J = 7.6 Hz), 6.867–6.785 (m, 6H), 5.761 (s, 1H, Ar-CH), 3.699 (s, 3H, OCH$_3$).

3,3′-*Bis*(*indolyl*)-4-*tertbutylphenylmethane* (**5h**) (*KBr, ν, cm*$^{-1}$): 3413 (NH), 3053, 2960, 2902, 2865, 1511, 1456 (C=N), 1416, 1338, 1092, 794, 742; ^{1}H NMR (400 Mz, DMSO-d_6) δ: 10.790–10.787 (d, 2H, NH), 7.343–7.280 (m, 8H), 7.039–7.002 (m, 2H), 6.871–6.836 (m, 4H), 5.778 (s, 1H, Ar-CH), 1.243 (S, 9H, C(CH$_3$)$_3$).

2-*Furyl*-3,3′-*bis*(*indolyl*)-*methane* (**5i**) (*KBr, ν, cm*$^{-1}$): 3407 (NH), 3115, 3052 (C–H, υ), 1455 (C=N), 1418, 1337, 1093, 1008, 783, 741 (NH, γ); ^{1}H NMR (400 Mz, CDCl$_3$) δ: 7.950 (s, 2H, NH), 7.489–7.469 (d, 2H, J = 8 Hz), 7.364–7.344 (m, 3H, J = 8 Hz, J = 0.8 Hz), 7.192–7.154 (m, 2H, J = 8 Hz, J = 0.8 Hz), 7.056–7.019 (m, 2H, J = 8 Hz), 6.878–6.873 (d, 2H, J = 2 Hz), 6.305–6.293 (m, 1H, J = 2 Hz), 6.061–6.053 (d, 1H), 5.942 (s, 1H, Ar-CH).

3,3′-*Bis*(*indolyl*)*styrylmethane* (**5j**) (*KBr, ν, cm*$^{-1}$): 3408 (NH), 3054 (C–H, υ), 3021, 2955 (CH, υ_{as}), 2914, 2849, 1456 (C=N), 1418, 1337, 1245, 1218, 1094, 742 (NH, γ); ^{1}H NMR (400 Mz, DMSO-d_6) δ: 10.889 (s, 2H, NH), 7.574–7.554 (d, 2H), 7.510–7.386 (m, 4H), 7.304–7.266 (t, 2H, J = 7.6 Hz), 7.194–7.190 (m, 3H), 7.092–7.055 (t, 2H, J = 7.6 Hz), 7.017–6.937 (m, 3H), 6.614–6,575 (d, 1H, J = 15.6 Hz), 5.391–5.371 (d, 1H).

4-*Hydroxylphenyl*-3,3′-*bis*(*indolyl*)*methane* (**5k**) (*KBr, ν, cm*$^{-1}$): 3446 (OH), 3403 (NH), 3053 (C–H, υ), 2957 (CH, υ_{as}), 2926, 2844, 1511, 1455 (C=N), 1257, 1172, 1088, 747 (NH, γ); ^{1}H NMR (400 Mz, DMSO-d_6) δ: 10.764–10.760 (d, 2H, NH), 9.130 (s, 1H, OH), 7.338–7.318 (d, 2H, [3]J = 8 Hz), 7.266–7.246 (d, 2H, [3]J = 8 Hz), 7.138–7.117 (d, 2H), 7.035–6.697 (m, 2H), 6.862–6.826 (m, 2H), 6.775–6.770 (d, 2H), 6.661–6.640 (m, 2H), 5.699 (s, 1H, Ar-CH).

2-*Hydroxylphenyl*-3,3′-*bis*(*indolyl*)*methane* (**5l**) (*KBr, ν, cm*$^{-1}$): 3409 (NH), 3054 (C–H, υ), 2955 (CH, υ_{as}), 1617, 1455 (C=N), 1093, 747 (NH, γ); ^{1}H NMR (400 Mz, DMSO-d_6) δ: 10.717 (s, 2H, NH), 9.346 (s, 1H, OH), 7.340–7.319 (d, 2H, [3]J = 8.4 Hz), 7.068–6,950 (m, 4H), 6.867–6.831 (t, 3H, [3]J = 7.2 Hz), 6.731 (s, 2H), 6.668–6.632 (t, 1H, [3]J = 7.2 Hz), 6.175 (s, 1H, Ar-CH).

2-*Hydroxyl*-3-*methoxyphenyl*-3,3′-*bis*(*indolyl*)*methane* (**5n**) (*KBr, ν, cm*$^{-1}$): ~3450 (OH), 3412 (NH), 3055 (C–H, υ), 2957 (CH, υ_{as}), 1509, 1456 (C=N), 1271, 1093, 745 (NH, γ); ^{1}H NMR (400 Mz, DMSO-d_6) δ: 10.753 (s, 2H, NH), 8.681 (s, 1H, OH), 7.346–7.326 (d, 2H, [3]J = 8 Hz), 7.298–7.278 (d, 2H, [3]J = 8 Hz), 7.045–7.007 (t, 3H, [3]J = 7.6 Hz), 6.960 (s, 1H), 6.876–6.839 (t, 3H, [3]J = 7.6 Hz), 6.803 (s, 2H, NHC*H*), 6.726–6.708 (d, 1H), 6.672–6.644 (d, 1H), 5.716 (s, 1H, Ar-CH), 3.661 (s, 3H, OCH$_3$).

3,3′-*Bis*(*indolyl*)*propane* (**5o**) (*KBr, ν, cm*$^{-1}$): 3409 (NH), 3053, 2957, 2927, 2869, 1455, 1477, 1337, 1093, 1010, 741; ^{1}H NMR (400 Mz, CDCl$_3$) δ: 7.882 (s, 2H, NH), 7.599–7.579 (d, 2H, [3]J = 8 Hz), 7.338–7.317 (d, 2H, [3]J = 8 Hz), 7.162–7.122 (m, 2H, [3]J = 8 Hz, [5]J = 0.8 Hz), 7.045–6.995 (m, 4H, [3]J = 8 Hz, [5]J = 0.8 Hz), 4.398–4.361 (t, 1H, Ar-CH, [3]J = 7.6 Hz), 2.287–2.213 (m, 2H, C*H*$_2$CH$_3$, [3]J = 7.6 Hz), 1.028–0.991 (t, 3H, CH$_2$C*H*$_3$, [3]J = 7.6 Hz).

3,3′-*Bis*(*indolyl*)*butane* (**5p**) (*KBr, ν, cm*$^{-1}$): 3408 (NH), 3386, 3058, 2955, 2926, 2869, 2849, 1455, 1418, 1369, 1339, 1095, 743, 736; ^{1}H NMR (400 Mz, CDCl$_3$) δ: 7.851 (s, 2H, NH), 7.605–7.585 (d, 2H, [3]J = 8 Hz), 7.327–7.307 (d, 2H, [3]J = 8 Hz), 7.158–7.121 (m, 2H), 7.047–7.008 (m, 2H), 6.984–6.979 (m, 2H), 4.510–4.473 (t, 1H, Ar-CH, [3]J = 7.6 Hz), 2.224–2.167 (m, 2H, [3]J = 7.6 Hz), 1.457–1.401 (m, 2H), 0.968–0.931 (t, 3H, [3]J = 7.6 Hz).

3,3′-*Bis*(*indolyl*)*isobutane* (**5q**) (*KBr, ν, cm*$^{-1}$): 3410 (NH), 3052, 2953, 2866, 1455, 1418, 1383, 1337, 1094, 1011, 782, 740; ^{1}H NMR (400 Mz, DMSO-d_6) δ: 10.721 (s, 2H, NH), 7.611–7.591 (d, 2H), 7.297–7.274 (m, 4H), 7.011–6.974 (t, 2H, [3]J = 7.2 Hz, [3]J = 7.6 Hz), 6.912–6.875 (t, 2H, [3]J = 7.6 Hz, [3]J = 7.2 Hz), 4.133–4.108 (d, 1H, [3]J = 9.6 Hz, Ar-C*H*CH), 2.718–2.659 (m, 1H, Ar-CHC*H*), 0.949–0.932 (d, 6H, CH$_3$).

3. Results and discussion

3.1. Acid contents and acidic strength of PSFSI/SBA-15

The acid loading and acid strength of PSFSI/SBA-15 are listed in Table 1. The acid contents were 0.87 and 0.90 mmol g^{-1} respectively for PSFSI$_1$/SBA-15 and PSFSI$_2$/SBA-15. Unfortunately, larger acid capacity failed to be achieved because agglomerate PSFSI appeared before the solvent was evaporated completely (PSFSI: SBA-15 = 1 g: 0.8 g). So, 0.90 mmol g^{-1} was believed to be the maximum content and using more PSFSI was unhelpful. Acid strength determined with the Hammett indicators showed that PSFSI$_1$/SBA-15 was strongly acidic. The results were accordant with our previous studies [20,21].

3.2. Characterization

The molecular weights of the homopolymers were determined by GPC. The tests were carried out after the samples were dissolved in water for 12 h. The sodium salt 4 had M_w = 40 900 and M_n = 13 000, and correspondingly, the value of PSFSI at the same

Table 1
Acid contents and acid strength of PSFSI/SBA-15.

Catalyst	Acid loading (mmol g^{-1})		Indicator and H_0		
	Tested	Calculated	Anthraquinone, −8.2	*p*-Nitrotoluene, −11.35	4-Chloronitrobenzene, −12.70
PSFSI$_1$/SBA-15	0.87	1.00	+	±	−
PSFSI$_2$/SBA-15	0.90	1.08	Untested		

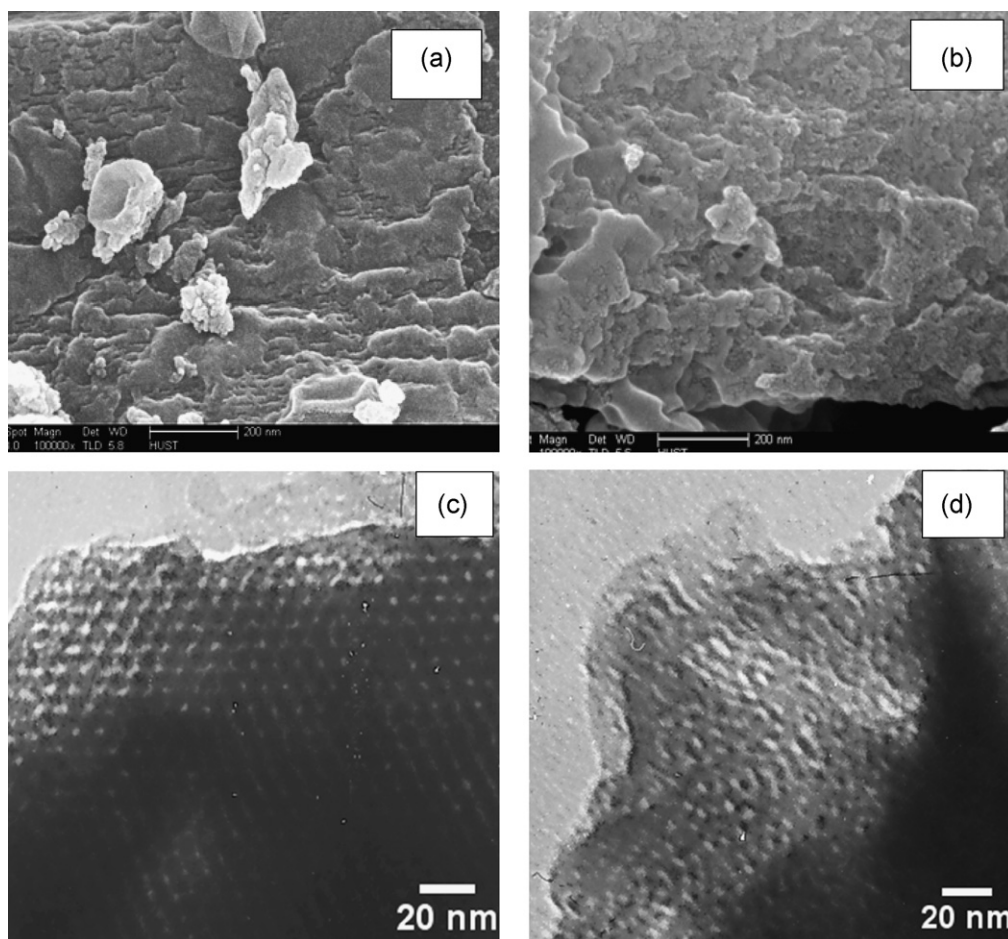(+), color changed clearly; (−), color unchanged; (±), color changed unclearly.

Fig. 3. SEM and TEM micrographs: (a) SEM for SBA-15, (b) SEM for PSFSI$_1$/SBA-15, (c) TEM for SBA-15 and (d) TEM for PSFSI$_1$/SBA-15.

order of magnitude. The PSFSI was not as hydroscopic as the monomer, p-CH$_2$=CHC$_6$H$_4$SO$_2$NHSO$_2$C$_4$F$_9$, and very convenient to be handled with in the air.

The linear homopolymer, PSFSI and the polymerisable monomer were identified with ^{1}H NMR and FT-IR. Fig. 1 presents the ^{1}H NMR spectra. In comparison of the spectrum of (b) with that of (a), the signals (6.828–5.374 ppm) of the vinyl group of **3** disappear. Correspondingly, the peaks of the polymer main chain (CH$_2$CH, 1.048–0.955) appear [27], and the chain protons of the remnant span-80 are also observed in spectrum (b). In the spectrum (c), the signals of NH appear (4.930 ppm).

The FT-IR spectra from 3200 to 400 cm^{-1} are shown in Fig. 2. It can be clearly seen that the characteristic absorption bands of the –SO$_2$– linkage (υ_{as} 1332 cm^{-1}, υ_s 1175 cm^{-1}) are in Fig. 2(c) [20,27,33]. Peaks at and 1141 cm^{-1} can be assigned to the symmetric C–F stretching vibration [33]. All the relevant peaks are not in SBA-15 spectrum at all in Fig. 2(b). The results confirm that PSFSI has been supported successfully.

SEM images clearly show that PSFSI is supported onto the surface of SBA-15 (Fig. 3(a) and (b)). Some accumulated particles of PSFSI dispersing on the external surface of support can be observed, which will damage the surface crystallinity of the samples.

The surface crystallinity-damage is accordant with the results detected by TEM (Fig. 3(c) and (d)). TEM images of SBA-15 clearly show that the hexagonal packing of the pores can be observed along the direction parallel to the pore axis (Fig. 3(c)). But as seen in Fig. 3(d), the integrity of mesoporous structure is not as regular as that of pure SBA-15, and some disorders appear.

XRD patterns of samples are shown in Fig. 4. The typical Bragg peaks in SBA-15 curve indicate the long-distance order of the hexagonal packing and peaks including (1 0 0), (1 1 0), and (2 0 0) reflection are obvious. A marked decrease in the diffraction intensity of the (1 0 0) reflection can be observed in PSFSI$_1$/SBA-15 curve, and the (1 1 0) and (2 0 0) peaks nearly disappear as well. The attenuation is just a reflection of a decrease of long-distance order and the surface mesoporous structure [25,34]. The disappearance of the (1 0 0) reflection in PSFSI$_2$/SBA-15 curve indicates that increasing loading leads to the loss of the orderly structure.

The thermal stability of samples was investigated by thermogravimetric analysis (TGA) and the results are shown in Fig. 5. Below 120 °C, the 5% weight loss in composite material (b) is due to the loss of incorporated water of the support (a) and no significant mass-loss is observed in PSFSI line (c). There are two main mass-loss stages in (c) line. One is between 223 and 310 °C and the other is between 310 and 378 °C, corresponding to the removal of –C$_4$F$_9$, and –SO$_2$NHSO$_2$ respectively. The tested mass-loss values of 47.7% and 39.8% nearly coincide with the calculated ones, 47.7% and 30.8% respectively. They are also discerned in the PSFSI$_1$/SBA-15 line. It is evident that compared with polystyrene-supported analogues in our previous studies [20,21], the PSFSI$_1$/SBA-15 achieves a significant improvement in thermal stability attributed to the more stable PSFSI (higher by 50 °C), and can be employed safely below 220 °C.

X-ray photoelectron spectroscopy analysis (XPS) is shown in Fig. 6. The peak at 290.9 eV of C1s signatures the –CF$_2$CF$_2$CF$_2$CF$_3$ group, and the F1s peak appears at 687.1 eV correspondingly. The N1s binding energy is found at 399.6 eV and S2p at 168.7 eV. The
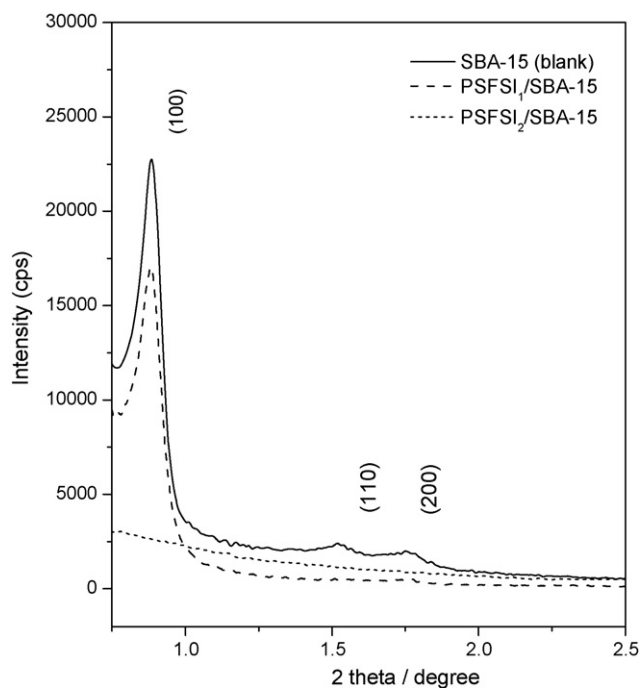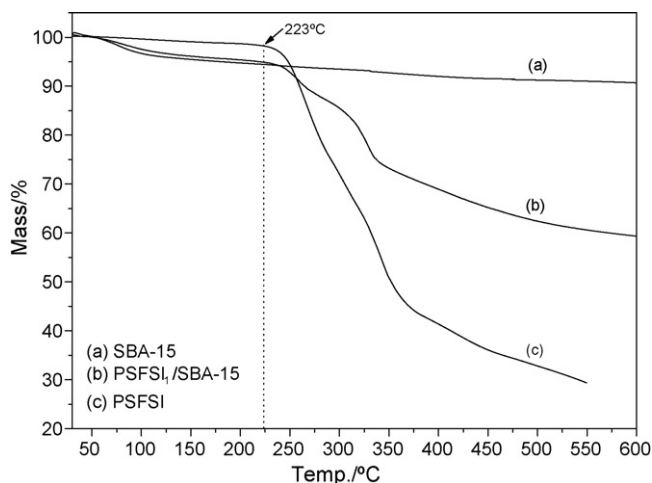
Fig. 4. XRD patters of samples.

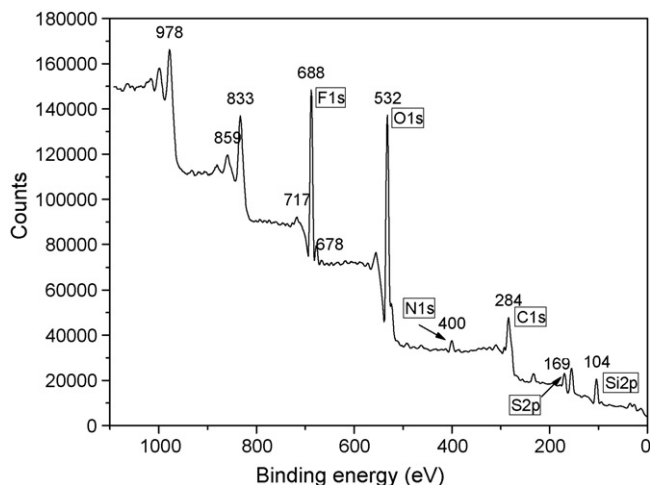**Fig. 5.** TGA analyses of samples: (a) pure SBA-15; (b) PSFSI$_1$/SBA-15; (c) PSFSI.

Fig. 6. XPS binding energy peaks of PSFSI/SBA-15.

Table 2
The catalytic performance of different catalysts for condensation of indole and benzaldehyde[a].

Entry	Catalyst	Amount of catalyst (mol%)	Time (h)	Yield (%)[b]
1	No cat.	0	24	53
2	PSFSI	5	3	87
3	NKC-9[c]	5	3	78
4	PSFSI$_1$/SBA-15	5	3	95
5	PSFSI$_1$/SBA-15	3	3	86
6	Amberlyst-15[d]	47	2.5	91
7	HY Zeolite[e]	12	2	82

[a] *Reaction conditions*: catalyst (0.87 mmol g^{-1}, relative to benzaldehyde), indole (4 mmol), benzaldehyde (2 mmol), stirred at 25–28 °C in 8 mL of CH$_2$Cl$_2$. The order of reagent addition was indole–catalyst–aldehyde.

[b] Isolated yield.

[c] NKC-9, –SO$_3$H resin, H_0 = −3.0.

[d] Data from Ref. [14]. 100 mg amberlyst-15 was used per mmol of benzaldehyde.

[e] Data from Ref. [5]. The total acidity value of the HY zeolite was 0.59 mmol g^{-1} and 200 mg was used per mmol of benzaldehyde.

peak found at 154.8 eV is attributed to Si2s while the peak at 104.0 eV is due to Si2p. The O1s binding energy is obviously found at 532.0 eV. The data show that PSFSI has been indeed supported on SBA-15.

3.3. PSFSI$_1$/SBA-15 catalyzed condensation of indole and aldehyde

Since DIMs had health-promoting properties, the condensation of indole and aldehyde was selected as a model reaction to assess the catalytic activities of the PSFSI$_1$/SBA-15.

Preliminary tests of the catalytic performance of PSFSI were carried out with indole and benzaldehyde as the substrates, and CH$_2$Cl$_2$ was selected as reaction solvent [5,6,14]. The results are listed in Table 2 and we can see that PSFSI itself shows a good catalytic activity for the reaction of indole with benzaldehyde. The DIM yield of 87% was superior to that for NKC-9 and comparable with those for Amberlyst-15 and HY Zeolite under similar reaction conditions with less catalyst, but accompanied by drastic swelling and poor recovery. The immobilization of homopolymer onto SBA-15 was anticipated to overcome this disadvantage. In fact, the PSFSI$_1$/SBA-15 could be recovered via simple filtration and showed better activity than PSFSI (Entry 4). Compared with Amberlyst-15, much less PSFSI$_1$/SBA-15 was needed to achieve almost same result (5 mol% vs. 47 mol%). Although decreasing the amount of the catalyst had some influence on the yield of the DIM, the activity of 3 mol% of PSFSI/SBA-15 was still satisfying (Entry 5). The superiority of PSFSI/SBA-15 could be attributed to the dispersed acid sites and higher acid strength.

In order to further examine catalytic performance of PSFSI$_1$/SBA-15 for other aldehydes, structurally diverse analogues were treated with indole under the conditions of 5 mol% of catalyst. The results are shown in Table 3 . All reactions proceeded smoothly to give the corresponding compounds in moderate to good yields, except for benzaldehyde containing a basic N(CH$_3$)$_2$ group at the *para* position (Entry 14).

The structure of the aldehydes had an obvious influence on the reaction. More quantity of aliphatic aldehydes (Entries 16–18) was required than that of aromatic ones to achieve desirable yields. The reaction of aromatic aldehydes was affected by substituents on the aromatic ring. The substrates with electron-withdrawing groups gave excellent yields (Entries 2–5), whereas most of the substrates with electron-donating groups gave relatively low yields, or required longer reaction time but the yield still satisfying except Entry 14 (Entries 6–15). It should be noted that the benzaldehyde containing the N(CH$_3$)$_2$ group gave poor yield, only 9%, even if the reaction time was extended to 7 h. We inferred that the alkalinity of the substituent deactivated the catalyst and this speculation was

Table 3
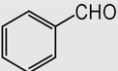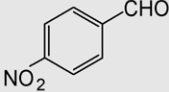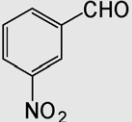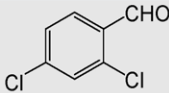PSFSI/SBA-15 catalyzed synthesis of DIMs[a].
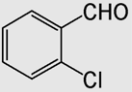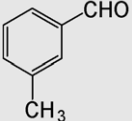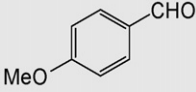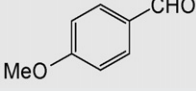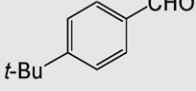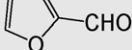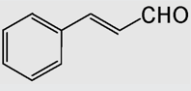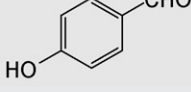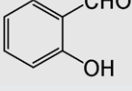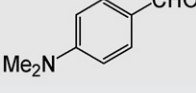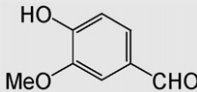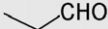
Entry	Aldehyde	Product	Time (h)	Yield (%)[b]
1		**5a**	3	95
2		**5b**	2	99
3		**5c**	2.5	94
4		**5d**	2.5	>99
5		**5e**	2	94
6		**5f**	4	84
7		**5g**	4	92
8[c]		**5g**	4	64
9		**5h**	4	88
10		**5i**	2	79
11		**5j**	2	69
12		**5k**	3.5	98
13		**5l**	4	74
14		**5m**	7	9

Table 3 (*Continued*)

Entry	Aldehyde	Product	Time (h)	Yield (%)[b]
15		**5n**	4	74
16		**5o**	4	90
17		**5p**	4	88
18		**5q**	4	94

[a] *Reaction conditions*: catalyst (0.87 mmol/g, 5 mol% relative to aldehyde), indole (4 mmol), aryl aldehyde (2 mmol), or alkyl aldehyde (3 mmol), stirred at 25–28 °C in 8 mL of CH_2Cl_2. The order of reagent addition was indole–catalyst–aldehyde.
[b] Isolated yield.
[c] An inverted order of reagent addition.

Table 4
Recycling results of $PSFSI_1$/SBA-15 in the model reaction of indole with 3-nitrobenzaldehyde.

Cycle	Yield (%)[a]
1	94
2	95
3	93
4	96
5	94

[a] Isolated yield.

confirmed by inverting the general order of adding reagents of aldehyde, catalyst and indole. 4-Methoxylbenzaldehyde was selected as a probing substrate and the yield of the DIM decreased from 92% to 64% (Entry 7 vs. 8). It was believed that the catalyst was partially poisoned for the weak alkalinity of the indole [5].

In order to check the reusability of $PSFSI_1$/SBA-15, 3-nitrobenzaldehyde was selectively used and the data are listed in Table 4. The results demonstrated that the $PSFSI_1$/SBA-5 had good recycling stability and could be used at least five times without obvious activity loss. The catalyst was readily recyclable and eco-friendly in the synthesis of DIMs.

4. Conclusions

By immobilizing the acidic homopolymer, poly(4-styrene-sulfonyl(perfluorobutylsulfonyl)imide)(PSFSI), onto SBA-15 silica, a new type of strongly acidic composite catalyst was developed. The composite catalyst was readily recyclable and eco-friendly in the condensation reactions of indole and aldehydes. It could be cycled five times without substantial decrease in activity, and proved to be highly efficient under mild conditions.

References

[1] C. Pal, S. Dey, S.K. Mahato, J. Vinayagam, P.K. Pradhan, V.S. Giri, P. Jaisankar, T. Hossain, S. Baruri, D. Ray, S.M. Biswas, Bioorg. Med. Chem. Lett. 17 (2007) 4924.
[2] C. Hong, G.L. Firestone, L.F. Bjeldanes, Biochem. Pharmacol. 63 (2002) 1085.
[3] V.T. Kamble, K.R. Kadam, N.S. Joshi, D.B. Muley, Catal. Commun. 8 (2007) 498.
[4] Farhanullah, A. Sharon, P.R. Maulik, V.J. Ram, Tetrahedron Lett. 45 (2004) 5099.

[5] M. Karthik, C.J. Mageshk, P.T. Perumal, M. Palanichamy, B. Arabindoo, V. Muruge-san, Appl. Catal. A 286 (2005) 137.
[6] M. Karthik, A.K. Tripathi, N.M. Gupta, M. Palanichamy, V. Murugesan, Catal. Commun. 5 (2004) 371.
[7] K. Tadi, Y. Chang, B.T. Ashok, Y. Chen, A. Moscatello, S.D. Schaefer, S.T. Schantz, A.J. Policastro, J. Geliebter, R.K. Tiwari, Biochem. Biophys. Res. Commun. 337 (2005) 1019.
[8] D.J. Faulkner, Nat. Prod. Rep. 18 (2001) 1.
[9] D.P. Chen, L.B. Yu, P.G. Wang, Tetrahedron Lett. 37 (1996) 4467.
[10] G. Babu, N. Sridhar, P.T. Perumal, Synth. Commun. 30 (2000) 1609.
[11] J.S. Yadav, B.V.S. Reddy, C.V.S.R. Murthy, G.M. Kumar, C. Madan, Synthesis (2001) 783.
[12] C. Manas, N. Ghosh, B. Ramkrshna, H. Yoshihiro, Tetrahedron Lett. 43 (2002) 4075.
[13] S.J. Ji, M.F. Zhou, D.G. Gu, Z.Q. Jiang, T.P. Loh, Eur. J. Org. Chem. (2004) 1584.
[14] C. Ramesh, J. Banerjee, R. Pal, B. Das, Adv. Synth. Catal. 345 (2003) 557.
[15] C.J. Magesh, R. Nagarajan, M. Karthik, P.T. Perumal, Appl. Catal. A: Gen. 266 (2004) 1.
[16] Z.H. Lin, C.J. Guan, X.L. Feng, C.X. Zhao, J. Mol. Catal. A: Chem. 247 (2006) 19.
[17] A.E. Feiring, S.K. Choi, M. Doyle, E.R. Wonchoiba, Macromolecules 33 (2000) 9262.
[18] K. Ishihara, A. Hasegawa, H. Yamamoto, Angew. Chem. Int. Ed. 40 (2001) 4077.
[19] B.H. Thomas, G. Shafer, J.J. Ma, M.H. Tu, D.D. DesMarteau, J. Fluorine Chem. 125 (2004) 1231.
[20] J. Xiao, Z. Zhang, J. Nie, J. Mol. Catal. A: Chem. 236 (2005) 119.
[21] Z. Zhang, S. Zhou, J. Nie, J. Mol. Catal. A: Chem. 265 (2007) 9.
[22] I.A. Koppel, R.W. Taft, F. Anvia, S.Z. Zhu, L.Q. Hu, K.S. Sung, D.D. DesMareau, L.M. Yagupolskii, Y.L. Yagupolskii, N.V. Ignat'ev, N.V. Kondratenko, A.Y. Volkonskii, V.M. Vlasov, R. Notario, P.C. Maria, J. Am. Chem. Soc. 116 (1994) 3047.
[23] D.D. DesMarteau, J. Fluoresc. Chem. 72 (1995) 203.
[24] M. Choi, W. Heo, F. Kleitz, R. Ryoo, Chem. Commun. (2003) 1340.
[25] M. Choi, F. Kleitz, D. Liu, H.Y. Lee, W.S. Ahn, R. Ryoo, J. Am. Chem. Soc. 127 (2005) 1924.
[26] H.J. Kim, H.J. Kweon, US Patent 0 113 530, 2005.
[27] T. Ishizone, J. Tsuchiya, A. Hirao, S. Nakahama, Macromolecules 25 (1992) 4840.
[28] J.L. Speier, J.A. Webster, G.H. Barnes, J. Am. Chem. Soc. 79 (1957) 974.
[29] M.A. Hofmann, C.M. Ambler, A.E. Maher, E. Chalkova, X.Y. Zhou, S.N. Lvov, H.R. Allcock, Macromolecules 35 (2002) 6490.
[30] K. Okuyama, X. Chen, K. Takata, D. Odawara, T. Suzuki, S. Nakata, T. Okuhara, Appl. Catal. A 190 (2000) 253.
[31] M. Fujiwara, K. Shiokawa, Y. Zhu, J. Mol. Catal. A: Chem. 264 (2007) 153.
[32] Q. Yang, J. Liu, J. Yang, M.P. Kapoor, S. Inagaki, C. Li, J. Catal. 228 (2004) 265.
[33] Y.K. Ke, H.R. Dong, Analytical Chemistry Handbook (third volume), Second Ed., Chemical Industry Press, Beijing, 1998, p. 965.
[34] N. Brodie-Linder, G. Dosseh, C. Alba-Simonesco, F. Audonnet, M. Impéror-Clerc, Mater. Chem. Phys. 108 (2008) 73.